Journal of The Electrochemical Society, **162** (4) A716-A721 (2015)
0013-4651/2015/162(4)/A716/6/$33.00

Model-Based Prediction of Composition of an Unknown Blended Lithium-Ion Battery Cathode

Z. Mao, M. Farkhondeh,* M. Pritzker,,z M. Fowler, Z. Chen, and M. Safari**

Department of Chemical Engineering, University of Waterloo, Waterloo, Ontario N2L 3G1, Canada

A model-based approach to accurately predict the composition of unknown blended Li-ion battery cathodes by fitting to experimental discharge curves is demonstrated. The electrochemically active constituents of the electrode are first determined by coupling information from low-rate galvanostatic lithiation data and SEM/EDX analyses of the electrode. The electrode composition is then estimated using a physics-based mathematical model of the electrode. The accuracy of this method has been assessed by comparison of the estimated composition with the value obtained from an independent, non-electrochemical experimental technique involving the deconvolution of XRD spectra. The electrode compositions obtained in these two ways are found to be in excellent agreement, within 1% of each other, demonstrating the promise of this new model-based approach. The method detailed in this work involves destructive and ex-situ testing, but only a relatively simple model is required to accurately determine the composition of a blended cathode in a Li-ion battery. This approach could also be useful for tracking the evolution of the blended electrode composition over the course of aging and gain a better understanding of the degradation mechanisms at play in cases where the active material loss contributes significantly to the overall capacity/power loss of the battery.

Manuscript submitted December 2, 2014; revised manuscript received January 14, 2015. Published February 5, 2015.

Lithium-ion batteries (LIBs) are promising devices for portable storage of energy. The high volumetric and gravimetric energy densities of these batteries have enabled them to surpass other alternatives such as Ni-Cd and Ni-MH batteries for applications such as cellular phones and lap-top computers. However, LIBs have still not achieved significant penetration into the automotive industry due to challenges associated with their safety, service life and cost.[1] This has led to considerable research interest both from chemists and engineers to improve the formulation of cell components and develop tools for design, performance assessment and durability improvement of the cell. Promising results regarding the overall improvement of electrode performance have been reported when the cathode is made up of a blend of oxides. Physical mixtures of layered oxides such as $LiNi_xMn_yCo_{1-x-y}O_2$ (NMC) or $LiNi_xCo_yAl_{1-x-y}O_2$ (NCA) with spinel $LiMn_2O_4$ (LMO) are good examples where the electrode performance benefits from a synergy between the individual components.[2–5] Not surprisingly, this has led to the increasing popularity of using blended cathodes in LIBs.[6]

Due to the complex nature of the phenomena associated with the operation of LIBs, their design and performance are best optimized and analyzed with the aid of mathematical models.[7] Such models have been developed for a broad range of purposes, from the estimation of kinetic and transport properties of the active material to the prediction of battery service life.[8–10] Few mathematical models have been reported in the literature which simulate the electrochemical behavior of known blended electrodes.[5,11–13] An open-circuit voltage model or "OCV model" has been used to estimate the mass ratios of two well-characterized insertion compounds, mainly $LiNi_{0.8}Co_{0.15}Al_{0.05}O_2$ and $LiMn_2O_4$ in Ref. 14, $LiNi_{1/3}Mn_{1/3}Co_{1/3}O_2$ and $LiAl_{0.1}Mn_{1.9}O_4$ in Ref. 11 and $LiNi_{1/3}Mn_{1/3}Co_{1/3}O_2$ and $LiMn_2O_4$ in Ref. 12. In such models, the blended cathode composition is estimated from differential capacity curves obtained from low-rate galvanostatic data (i.e., quasi-equilibrium condition). In this approach, the capacity of the blended electrode (i.e., inverse of the quasi-equilibrium curve as a function of capacity) is related to those of the individual active compounds as a function of potential through a summation weighted linearly according to their mass ratios. Although this method is relatively straightforward, it does not account for possible interactions that can occur between the active compounds. In studies where it was used to predict the composition of blended cathodes with known composition, its estimation error was found to be approximately 6%.[11,14] Furthermore, this procedure becomes more difficult and less accurate when the identity of the active compounds is not well known. The need to quantitatively assess the performance of LIBs with unknown electrode formulations is becoming ever more important given the increasing popularity of introducing batteries with blended cathodes into the commercial market.

In this communication, a systematic procedure is followed to determine the composition of an unknown blended electrode with an acceptable accuracy less than ~1% error that is validated with ex-situ measurements. The cathode morphology and its elemental composition are first characterized using scanning electron microscopy (SEM) and energy-dispersive X-ray (EDX) analyses, respectively. The electrochemically-active components of the cathode are then identified by analysis of experimental electrode galvanostatic discharge data obtained at a very low current. In the next step, a physics-based model of the blended cathode is fitted to the galvanostatic lithiation curve to estimate the electrode composition. Finally, the prediction of the proposed model-based method is validated against a calibration curve obtained by independent and purely experimental X-ray diffraction (XRD) measurements. Accordingly, the cathode composition is determined in a non-destructive way once the component oxides are identified. It is important to emphasize that the objective of the model used in this procedure is not to describe lithiation and delithiation of the cathode under all conditions. Instead, this model is intended only to estimate the composition of the blended cathode. By choosing to apply this method to discharge data obtained at very low current, a relatively simple model can be used since porous electrode effects can be neglected. Although this procedure is demonstrated on discharge data, it could equally well be applied to a blended cathode during charging.

Experimental

In this study, standard 2-electrode experiments were conducted on coin cells assembled in our laboratory that contained cathodes made of an oxide blend with unknown composition. The blended cathode was received in the form of a double-side-coated rectangular electrode sheet (225 mm × 164 mm) with aluminum as the current collector. Circular pieces (1.013 cm^2 in area) were cut from this sheet for use in the coin cells that were characterized in the various ways described below. For the electrochemical tests, one side of the coating was wiped off carefully using N-methyl-2-pyrolidinone (NMP). Each coin cell was assembled by placing a Celgard 2500 sheet soaked in an electrolyte containing 1 M $LiPF_6$ dissolved in a 1:1(wt) EC/DMC between a circular blended cathode piece and a Li counter/reference electrode. The electrode preparation and cell assembly were performed inside an argon-filled glove box. A series of reference samples were prepared for XRD characterization by mixing together the identified (i.e., using

*Electrochemical Society Student Member.
**Electrochemical Society Active Member.
zE-mail: pritzker@uwaterloo.ca

a procedure described later in this communication) active-material components of the unknown cathode. The reference insertion compounds were purchased from Sigma-Aldrich in the form of powder and mixed together in different proportions using a ceramic mortar and pestle.

The morphological and elemental analyses of the cathodes were performed by SEM and EDX (Zeiss). XRD (XRG300 with Cu Kα radiation) was used to characterize the crystal structure of the unknown cathode and reference samples and identify the phases present. Galvanostatic experiments were conducted on the coin cells using a battery cycler (Neware CT-3008-5 V10 mA-164-U) operating under constant-current conditions between the lower and upper cutoff potentials of 3 and 4.2 V, respectively. Each cell was first subjected to 5 formation cycles, each of which consists of two-step charge and discharge segments under constant current. A constant current of C/2 was used in the first step followed by C/100 in the second step. The purpose of the second step was to ensure that the electrode was fully lithiated by the end of the discharge step and fully delithiated by the end of charging. At the end of the 5 formation cycles, the fully-charged blended cathode was lithiated at a rate of C/25.

Model

A simple physics-based model is used to simulate the galvanostatic discharge of the unknown blended cathode under low current. As noted in the Introduction, porous electrode effects are neglected since the model is being applied to data obtained at low C-rates. Such an assumption has been shown previously to be acceptable for low C-rate conditions up to 1C in typical electrode designs.[15–18] According to this assumption, the active particles are connected to a uniform sink or source of electrons (i.e. a conductive matrix) and Li^+ ions in the electrolyte. The blended cathode is assumed to be made of a physical mixture of N total types of active materials. Each type n of the active materials is present as a spherical particle with radius R_n within which Li diffuses, as described in Eqs. 1–3 below:

$$\frac{\partial c_n}{\partial t} = \frac{1}{r^2}\frac{\partial}{\partial r}\left(D_n r^2 \frac{\partial c_n}{\partial r}\right), \quad [1]$$

$$\left.\frac{\partial c_n}{\partial r}\right|_{r=0} = 0, \quad [2]$$

$$\left.\frac{\partial c_n}{\partial r}\right|_{r=R_n} = -\frac{i_n}{F D_n}, \quad [3]$$

where c_n and D_n are the concentration and diffusion coefficient, respectively, of lithium within the active particles of type n. i_n is the current density over the active surface area of the particles of type n and is related to the cathode potential Φ according to the following form of the Butler-Volmer equation:

$$i_n = F k_n \sqrt{c_e}\sqrt{c_n^{max} - c_n^s}\sqrt{c_n^s}\left\{\exp\left(\frac{0.5F}{RT}(\Phi - U_n)\right) - \exp\left(-\frac{0.5F}{RT}(\Phi - U_n)\right)\right\}, \quad [4]$$

where U_n is the equilibrium potential evaluated according to the lithium concentration c_n^s at the particles surfaces, c_n^{max} is the maximum lithium concentration and k_n is the rate constant for the charge-transfer reaction at the surface of the n^{th} particle type. Finally, c_e, T, F and R are the electrolyte concentration, temperature, Faraday constant and gas constant, respectively. It should be noted that the potential distributions in the electrolyte and the electrode are neglected under the very low current condition used in our simulations and, thus, Φ corresponds to the cell potential vs. Li reference electrode.

The total current I_t is distributed over all the N types of particles as follows:

$$3M_t \sum_{n=1}^{N} \frac{\varepsilon_n i_n}{\rho_n R_n} = I_t, \quad [5]$$

where ρ_n is the density of the n^{th} type of particles and ε_n is the mass fraction of the n^{th} type of particles with respect to the total mass M_t of active material in the electrode and is subject to the condition:

$$\sum_{n=1}^{N} \varepsilon_n = 1 \quad [6]$$

The overall capacity Q of the blended electrode is related to the capacity q_n of the n^{th} type of particles and their mass fractions in the electrode as follows:

$$M_t \sum_{n=1}^{N} \varepsilon_n q_n = Q \quad [7]$$

In this expression, q_n is the practical mass-specific capacity of the n^{th} type of active compound, which generally is an empirical value depending on the material synthesis method and the operating voltage range. q_n is obtained from the literature in accordance with a voltage range of 3 V to 4.2 V and is listed in Table II.

The governing equations were solved using the COMSOL Multiphysics 4.2 simulation package with a particle domain (i.e., one-dimensional) discretized into 20 equal intervals in the radial direction. The same formulation presented here can be used without any modification for the simulation of the dynamic behavior of the cell under low to medium applied currents. In this case, the solid-state diffusion and the surface resistance due to charge transfer will contribute to the capacity and potential loss of the electrode. If ionic and electronic transport effects at the electrode scale are explicitly included, the assumption of negligible porous electrode effects is relaxed and the resulting pseudo-2D model[19] can be used to simulate the discharge behavior at high rates. However, as noted previously, this is not required to estimate the blended cathode composition according to the procedure described in the following sections.

Results

Surface morphology and elemental composition of the unknown cathode.— The surface of the unknown cathode was examined by SEM and EDX. Figure 1 shows an SEM image of a portion of the electrode surface showing the presence of two different types of particle agglomerates/clusters within the electrode. The first group (denoted as NO.1) is made of a few particles with dimensions ranging from 1–2 μm whereas the second group (denoted as NO.2) is composed of

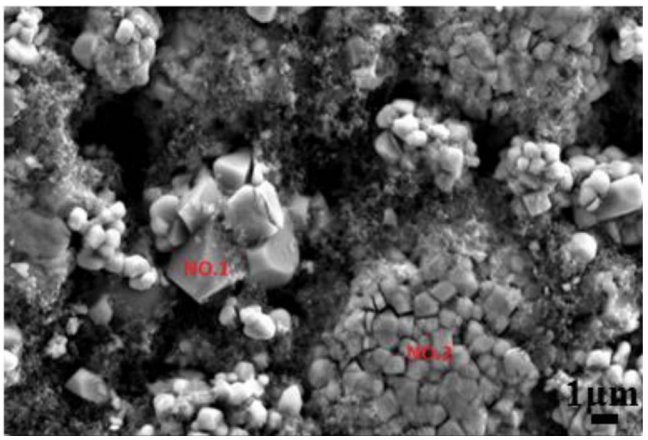

Figure 1. SEM image of the unknown cathode surface. EDX analysis was conducted on the two groups of particles labeled NO.1 and NO.2 above.

Table I. EDX analysis of elemental composition of the unknown cathode corresponding to zones NO.1 and NO.2 in Figure 1.

		O	Co	Ni	Mn
atomic %	group NO.1	61.12	0.15	0.28	26.05
	group NO.2	58.25	6.53	5.98	9.34

many particles smaller than 1 μm. The particle size distributions for both particle groups obtained from SEM image analysis are found to obey log-normal distribution functions yielding a d_{50} of 1.74 μm for group NO.1 and 0.87 μm for group NO.2. The results of the elemental analysis of these two particle groups are summarized in Table I. O, Mn, Co and Ni are found to be present in both groups. Not surprisingly, O is a dominant element in both groups. Among the metals, Mn is the major element in group NO.1, while the composition is more evenly split among Mn, Ni and Co in group NO.2. This preliminary analysis suggests that the active materials in the electrode are composed of two types of metal oxides: the first type is likely a Mn-oxide (i.e. LMO), while the second one is likely a mixed-oxide with nearly equal atomic fractions of Ni, Mn and Co (i.e. NMC).

Active material components of the unknown cathode.— The discharge profile of the unknown-cathode/Li cell at a current corresponding to C/25 is presented in Figure 2a. The discharge capacity of this cell is found to be approximately $Q_{C/25} = 2$ mAh. The discharge profile is presented in terms of the normalized capacity Q_{norm} (i.e., with respect to the end-of-discharge capacity) defined as:

$$Q_{\text{norm}} = \frac{Q}{Q_{C/25}} \quad [8]$$

This enables the intrinsic electrochemical signature of the electrode to be more easily compared to those of known individual active materials reported in the literature. The differential capacity is a property that can effectively delineate the subtle electrochemical changes of the electrode over the course of lithiation/delithiation. Accordingly, plots of differential capacity versus electrode potential provide rich information about the active materials in a given electrode.[20] Typically, at least one peak appears in these plots for the active materials used in LIBs. The potentials at which peaks appear are unique for a given active material and so potentially can be used to identify the components of a mixed electrode.[11,14] Figure 2b presents the differential capacity plot of the unknown cathode that has been determined from the electrode discharge data obtained at C/25 and shown in Figure 2a. Three distinct peaks at 3.743, 4.005 and 4.136 V appear in the plot. Based on the SEM/EDX results in the previous subsection, one should be able to match the three peaks in Figure 2b with those of a Mn-oxide and a Mn-Co-Ni mixed oxide. However, different varieties of active materials composed of these metals have been reported in the literature. We examined different candidates from the literature by comparing their differential capacity signatures to that of our unknown cathode. The first peak at 3.743 V closely matches that observed for $LiNi_{1/3}Mn_{1/3}Co_{1/3}O_2$ denoted here as NMC,[21] whereas the other two peaks at 4.005 and 4.136 V correspond well to $LiMn_2O_4$ denoted as LMO[5] (see Figure 2c). This agreement provides strong support for the results obtained from the SEM and EDX analysis.

Model-based composition estimation of the unknown cathode.— In the previous section, LMO and NMC were identified as the active compounds in the unknown cathode. Here, the mathematical model introduced earlier is used to simulate the discharge curves from which the composition of the unknown cathode can be determined. The list of model parameters used in the simulations is presented in Table II. In the solid phase, a constant diffusion coefficient for LMO is used with a slight adjustment based on Ref. 5, while a variable diffusion coefficient for NMC that depends on the Li content is fitted in accordance with open-circuit-relaxation analysis in Ref. 21. The equilibrium potentials U_n for LMO and NMC have been obtained from Ref. 5 and Ref. 21, respectively, to be within the operating potential window of 3 V–4.2 V used in this study. Accordingly, given the theoretical capacities and assuming both active materials are fully-lithiated at the potential of 3 V, Li stoichiometry is determined to vary from 0.35 to 1 in LMO and from 0.457 to 1 in NMC in the blended cathode of our study. It should be noted that C/25 conditions were considered in Refs. 5 and 21 to be slow enough that the potentials measured during discharge approximate the open-circuit potentials and, thus, are suitable equilibrium potentials of the individual compounds. With these values as well as the reaction rate constant and solid-state diffusion coefficient known from the literature, the only unspecified parameters are the total active material loading M_t and the mass fractions ε_n of the two active materials. The model can then be used to simulate the discharge profiles for different arbitrarily-set values of ε_n and the corresponding M_t obtained from Eq. 7 to yield the values shown in Table III. Figure 3 presents the simulated LMO–NMC blended cathode discharge profiles (dashed lines) obtained at C/25 for 11 NMC compositions at equal intervals between 0 wt% and 100 wt%. The experimental discharge profile (solid line) of the unknown cathode is superimposed in Figure 3 to compare with the model-computed curves. It should be emphasized that no parameters have been adjusted to fit the model to the measured discharge curve and the computed and experimental curves are simply overlaid together. The comparison clearly shows that the simulation corresponding to a NMC composition of 70 wt% provides a very close match to the experimental data.

X-ray-based composition refinement of the unknown cathode.— In order to validate the model prediction, an X-ray-based method is used to estimate the composition of the unknown cathode. This method is

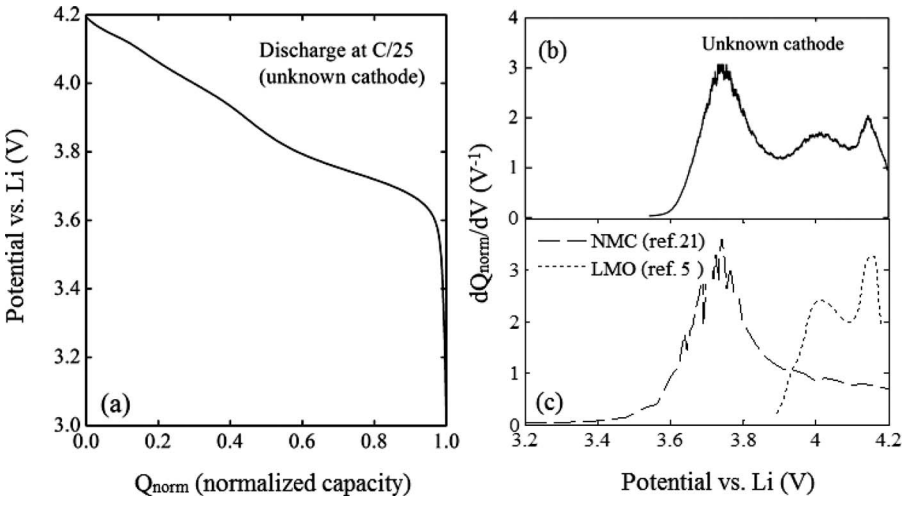

Figure 2. (a) Experimental potential-Q_{norm} profile and (b) corresponding experimental differential capacity signature of the unknown cathode/Li cell discharged at current C/25. (c) Differential capacity profiles of LMO and NMC electrodes corresponding to the equilibrium potentials reported in Refs. 5 and 21, respectively.

Table II. List of model parameters.

Parameter	Symbol	LMO	NMC
Number of particle groups	N	2	
Faraday constant (C mol^{-1})	F	96478	
Gas constant (J mol^{-1} K^{-1})	R	8.314	
Temperature (K)	T	298	
Electrolyte concentration (mol m^{-3})	c_e	1000[m]	
Radius of type n particle (μm)	R_n	0.87[m]	0.435[m]
Capacity of unknown cathode (Ah)	Q	0.002[m]	
Density of type n particle (kg m^{-3})	ρ_n	4220	4770
Capacity of type n particle (Ah kg^{-1})	q_n	100[5]	150[21]
Maximum lithium concentration in type n particle (mol m^{-3})	c_n^{max}	23339[5]	49761[21]
Rate constant of charge transfer reaction on type n particle surface (mol/[m^{2}s(mol m^{-3})$^{1.5}$])	k_n	5×10^{-10}[5]	1×10^{-10}[5]
Diffusion coefficient of Li in type n particle (m^2 s^{-1})	D_n	6.6×10^{-15}[5]	$1.25\ 10^{-13}\ y^2 - 2.68\ 10^{-13}\ y + 1.44\ 10^{-13}$ (y is coefficient in $Li_yNi_{1/3}Mn_{1/3}Co_{1/3}O_2$)[21]

[m]Measured or based on experimental conditions.

Table III. Calculated total active material loading M_t for the mass fractions ε_n used in the simulations.

Parameter	Values										
ε_1	0	0.1	0.2	0.3	0.4	0.5	0.6	0.7	0.8	0.9	1.0
ε_2	1.0	0.9	0.8	0.7	0.6	0.5	0.4	0.3	0.2	0.1	0
M_t(mg)	13.3	13.8	14.3	14.8	15.4	16.0	16.7	17.4	18.2	19.0	20.0

based on the concept that the composition of a mixture of crystalline phases in a sample can be determined from the relative areas under their characteristic diffraction peaks. Accordingly, a calibration curve consisting of a plot of the ratio of the areas under the characteristic XRD peaks associated with the two components in a LMO–NMC mixture versus the mixture composition was prepared. To obtain such a calibration curve, pure LMO and NMC powders from Sigma Aldrich were mixed in different mass ratios (i.e., 20%, 40%, 60%, 80% NMC) and the XRD patterns of these mixtures together with those of pure LMO and NMC powders were obtained. For this purpose, the evolution of the relative XRD peak intensities corresponding to the (101) plane ($R\bar{3}m$ space group) for NMC and the (311) plane ($Fd3m$ space group) for LMO was used for all compositions.[22–24] The experimental XRD patterns for the four samples composed of 20 to 80 wt% NMC are presented in Figure 4. Figures 4a–4d clearly show that the (101) NMC peak grows at the expense of the (311) LMO peak as the weight percentage of NMC in the mixture increases. The pseudo-Voigt function is fitted to each of the patterns in Figures 4a–4d to approximate the area under each peak. The ratio of the area under the (101) NMC peak to the area under both (101) NMC and (311) LMO peaks is plotted versus the weight fraction of NMC in the NMC–LMO mixture in Figure 5 (circles). The cubic function below (Eq. 9) has been found to fit the experimental data very well and is also included in Figure 5 (dashed line) so that the composition of any unknown mixture of NMC and LMO can be estimated from the XRD data:

$$y = -1.6x^3 + 2.3x^2 + 0.34x + 0.0007 \quad [9]$$

where x is the ratio of the area under the (101) NMC peak to the area under both (101) NMC and (311) LMO peaks and y is the weight fraction of NMC in the NMC–LMO mixture.

The XRD diffractogram of the unknown blended cathode is presented in Figure 6. The inset shows the diffraction pattern magnified between 35° and 38° (solid line) and the pseudo-Voigt functions fitted to the (101) NMC and (311) LMO peaks (dashed lines). From the areas under these peaks obtained from the pseudo-Voigt fits and the calibration curve in Figure 5, the composition of the unknown cathode is estimated to be 71 wt% NMC. This composition is very close to the one predicted by the model-based method (i.e., 70%). This level of agreement between the two methods indicates that the simple model-based approach proposed in this study is of acceptable accuracy and should prove valuable as a versatile technique for determination of the composition of unidentified blended electrodes. One reason for the very good level of agreement achieved using the physic-based

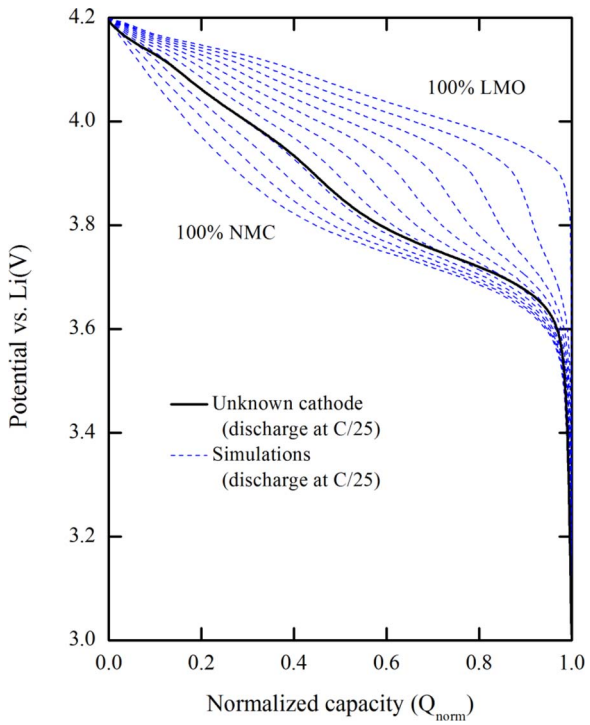

Figure 3. Experimental discharge profile (solid line) of unknown cathode at C/25 and simulated discharge profiles (dashed lines) of a LMO-NMC blended-cathode discharge at C/25 for 11 NMC compositions at equal intervals between 0 and 100 wt%.

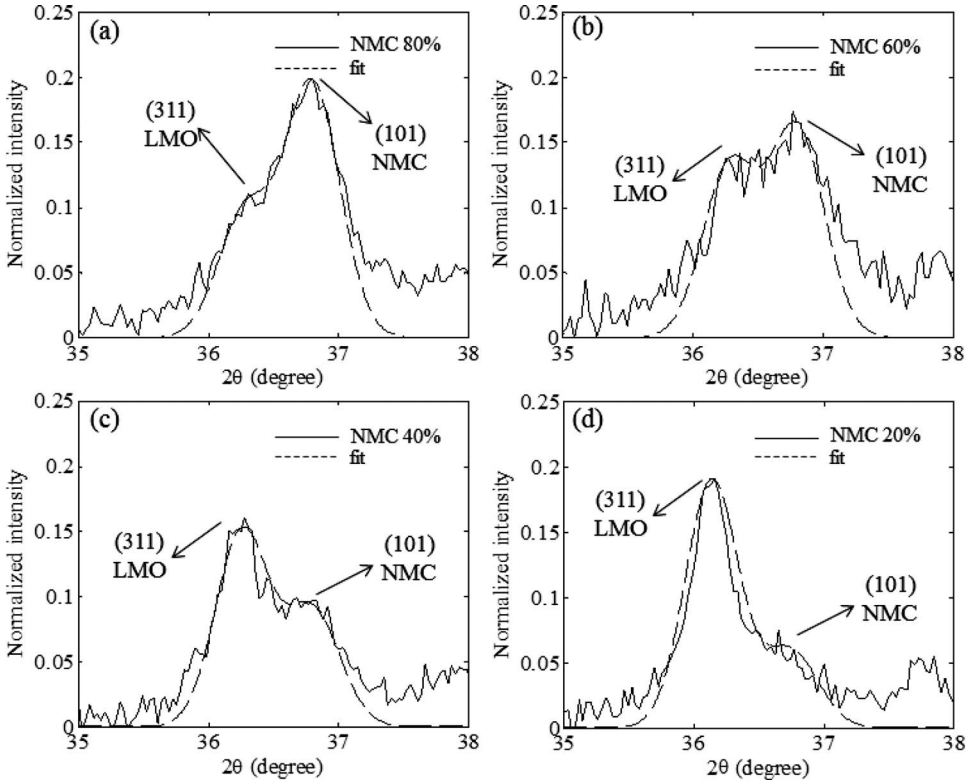

Figure 4. Experimental XRD patterns (solid lines) of NMC-LMO powder mixtures with compositions (a) 80, (b) 60, (c) 40 and (d) 20 wt% NMC and pseudo-Voigt fitted patterns (dashed lines) of (101) NMC and (311) LMO peaks for 2θ between 35° and 38°.

model may be that it is able to capture interactions between the active compounds by considering the particles to be connected to each other in parallel at every location across the electrode so that they remain at the same electric potential throughout lithiation/delithiation regardless of the rate condition. If the particles have the same chemistry (i.e., identical equilibrium potential curves), they will have identical Li-content; however, if the particles have different chemistries, they will be lithiated/delithiated to different extents at any particular time depending on their equilibrium potentials. Possible interactions between active components are not considered in the previous OCV models in which the differential capacity curve of the blended cathode is obtained through a linear combination of the OCVs of the individual compounds weighted according to their mass ratios. The error associated with the OCV models[11,12,14] would likely diminish if the actual equilibrium potentials (i.e., potential of the relaxed electrode under open-circuit condition) rather than the quasi-equilibrium potentials (i.e., C/25 galvanostatic discharge curve) were being measured because the interactions between the active compounds disappear

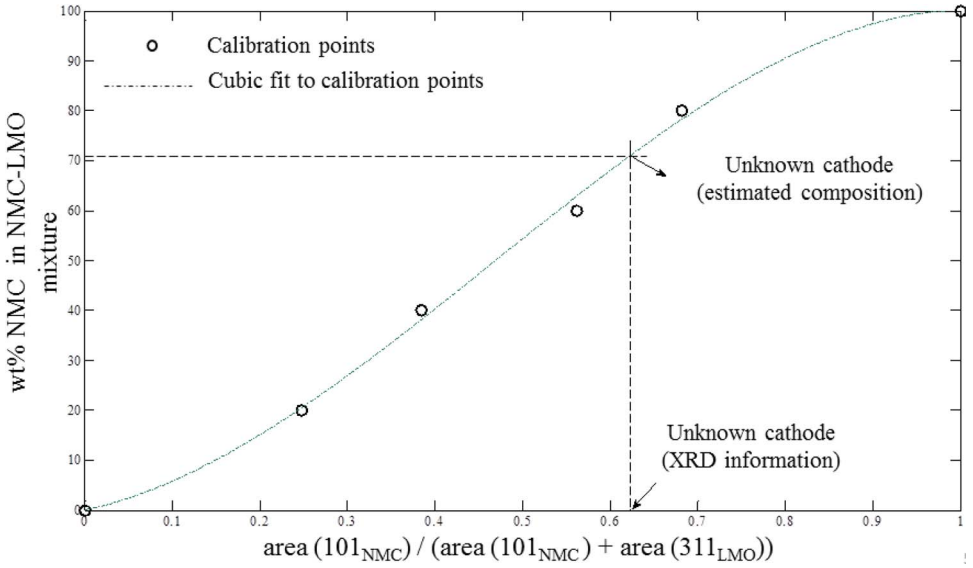

Figure 5. XRD-based calibration plot (circles and dotted line) correlating the ratio of the area under (101) NMC peak to the area under both (101) NMC and (311) LMO peaks to wt% NMC in a NMC-LMO mixture.

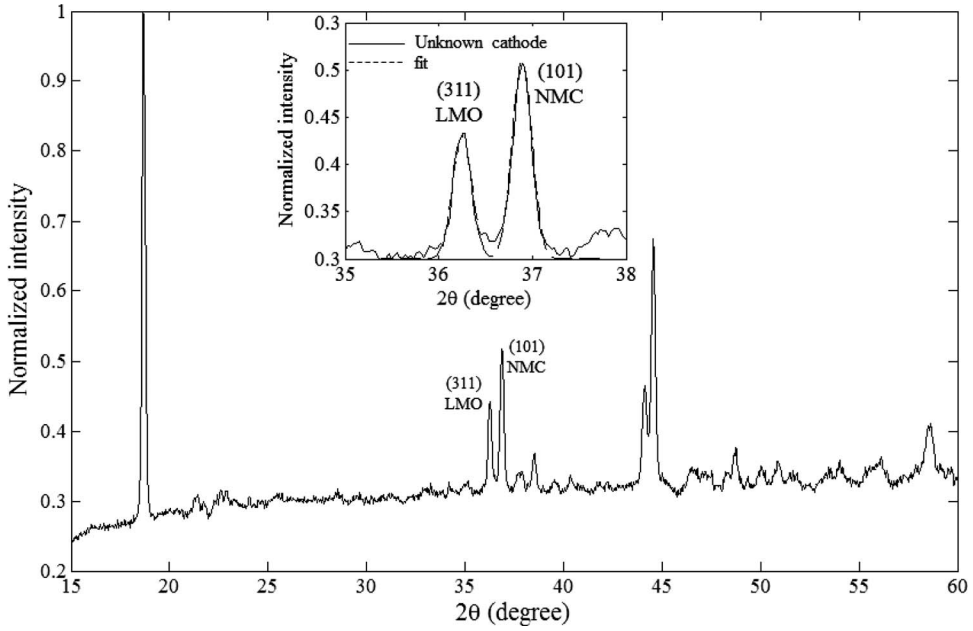

Figure 6. XRD pattern of unknown blended cathode. The portion of the pattern and the pseudo-Voigt fit of the (101) NMC and (311) LMO peaks (dashed line) are shown at higher resolution over the 2θ range between 35° and 38° in the inset.

under this condition. Although C/25 condition is slow enough for the galvanostatic potential-capacity curve to approximate the equilibrium potential of a single active-compound electrode, care must be taken in making such an assumption for an electrode containing two or more different active chemistries.

Conclusions

An effective method for composition estimation of blended cathodes is proposed and validated for a NMC-LMO blended cathode. The method consists of two main steps. In the first step, SEM/EDX analysis and the differential capacity signature of the sample are used to identify the active materials. A physics-based model is then used to simulate the electrode discharge at a very low current (e.g. C/25) and compare to the experimental discharge profile in order to estimate the electrode composition. The model prediction is found to be in excellent agreement with the composition obtained from an independent, non-electrochemical experimental technique, i.e., powder X-ray diffraction of the identified commercial compounds. Although the procedure is demonstrated on discharge profiles in this study, it could be equally well applied to charge data. The approach detailed in this work includes destructive and ex-situ testing, but only a relatively simple model is required to accurately determine the composition of a blended cathode in a Li-ion battery. The high level of accuracy of this model-based approach should also make it useful for tracking the evolution of the blended electrode composition over the course of aging in cases where active material loss (e.g., dissolution) along with other degradation mechanisms contribute to the overall capacity/power loss of the battery.

Acknowledgment

The authors are indebted to the General Motors Co., Automotive Partnership Canada (Project APCPJ 395996-09) and the Natural Sciences and Engineering Research Council of Canada (Project RGPIN-170912) for their financial support to carry out this work.

References

1. J. B. Goodenough and K.-S. Park, *Journal of the American Chemical Society*, **135**(4), 1167 (2013).
2. J. Gao and A. Manthiram, *Journal of Power Sources*, **191**(2), 644 (2009).
3. H. Y. Tran, C. Taubert, M. Fleischhammer, P. Axmann, I. Kuppers, and M. Wohlfart-Mehrens, *Journal of The Electrochemical Society*, **158**(5), A556 (2011).
4. K.-S. Lee, S.-T. Myung, Do.-W. Kim, and Y.-K. Sun, *Journal of Power Sources*, **196**(16), 6974 (2011).
5. P. Albertus, J. Christensen, and J. Newman, *Journal of The Electrochemical Society*, **156** (7), A606 (2009).
6. S. B. Chikkannanavar, D. M. Bernardi, and L. Liu, *Journal of Power Sources*, **248**, 91 (2014).
7. J. Newman, K. E. Thomas, H. Hafezi, and D. R. Wheeler, *Journal of Power Sources*, **119**, 838 (2003).
8. J. Newman, *Journal of The Electrochemical Society*, **142**(1), 97 (1995).
9. S. Stewart and J. Newman, *Journal of The Electrochemical Society*, **155**(6), A458 (2008).
10. C. Delacourt and M. Safari, *Journal of The Electrochemical Society*, **159**(8), A1283 (2012).
11. T. Kobayashi, N. Kawasaki, Y. Kobayashi, K. Shono, Y. Mita, and H. Miyashiro, *Journal of Power Sources*, **245**, 1 (2014).
12. S. Jung, *Journal of Power Sources*, **264**, 184 (2014).
13. Y. L. Dai, L. Cai, and R. E. White. *Journal of Power Sources*, **247**, 365 (2014).
14. J. P. Schmidt, H. Y. Tran, J. Richter, E. Ivers-Tiffee, and M. Wohlfahrt-Mehrens, *Journal of Power Sources*, **239**, 696 (2013).
15. S. Santhanagopalan, Q. Guo, P. Ramadass, and R. E. White, *Journal of Power Sources*, **156**(2), 620 (2006).
16. M. Safari and C. Delacourt, *Journal of The Electrochemical Society*, **158**(2), A63 (2011).
17. M. Farkhondeh and C. Delacourt, *Journal of The Electrochemical Society*, **159**(2), A177 (2012).
18. M. Farkhondeh, M. Safari, M. Pritzker, M. Fowler, T. Han, J. Wang, and C. Delacourt, *Journal of The Electrochemical Society*, **161**(3), A201 (2014).
19. M. Doyle, T. F. Fuller, and J. Newman, *Journal of The Electrochemical Society*, **140**(6), 1526 (1993).
20. A. H. Thompson, *Journal of The Electrochemical Society*, **126**(4), 608 (1979).
21. S.-L. Wu, W. Zhang, X. Song, A. K. Shukla, G. Liu, V. Battaglia, and V. Srinivasan, *Journal of The Electrochemical Society*, **159**(4), A438 (2012).
22. N. Yabuuchi, Y. Makimura, and T. Ohzuku, *Journal of The Electrochemical Society*, **154**(4), A314 (2007).
23. Y. Koyama, I. Tanaka, H. Adachi, Y. Makimura, and T. Ohzuku, *Journal of Power Sources*, **119**, 644 (2003).
24. M. M. Thackeray, P. J. Johnson, L. A. de Picciotto, P. G. Bruce, and J. B. Goodenough, *Materials. Research. Bulletin*, **19**(2), 179 (1984).